Discrete Element Modelling of Large Scale Stacked-Ring Simple Shear Test of Steel Spheres

Nina Zabihi[1] and Adda Athanasopoulos-Zekkos, Ph.D.[2]

[1]Ph.D. Candidate, Dept. of Civil and Environmental Engineering, Univ. of Michigan, Ann Arbor. E-mail: ninazbh@umich.edu
[2]Associate Professor, Dept. of Civil and Environmental Engineering, Univ. of Michigan, Ann Arbor. E-mail: addazekk@umich.edu

ABSTRACT

Traditionally, geotechnical engineers have used continuum numerical methods coupled with complex constitutive models to analyze soil response. This approach, however, does not explicitly consider the particle-scale interactions underlying the macro-scale behavior. Given the advances in computational power, particle-based discrete element methods have been progressively catching the attention of geotechnical engineers in simulating and analyzing soil behavior. For validation of discrete element modeling of various laboratory tests, many researchers have been using idealized granular materials such as steel spheres that are much simpler to model compared to real soils. In case of experimental validation of models for simple shear test using stacked-ring device type, it is particularly important to ensure that the simple shear condition is completely imposed on specimens consisting of low friction and freely rotating steel spheres. In this study, discrete element modeling is used to examine the level of simple shear imposition on specimen of uniform-sized steel spheres in large scale stacked-ring simple shear device under constant volume conditions.

INTRODUCTION

Understanding the behavior of soils under simple shear conditions is very important in a large number of geotechnical engineering problems such as earthquakes, slope stability, and pile driving. Direct simple shear device is one of the commonly used experimental devices to study such behavior of soil that is believed to be capable of reproducing the field loading conditions which particularly involve the rotation of principal stress axes during plane-strain shearing (Boulanger et al. 1993; Budhu 1988). This device has been used by several researchers for studying the monotonic and cyclic response of sands, silts, and clays (e.g., Vaid and Chern 1985; Vucetic and Dobry 1988; Wijewickreme 2010). However, there are limited simple shear test data available for gravels (e.g., Chang et al. 2014; Hubler et al. 2017) as larger devices are needed for studying their simple shear behavior.

There are three commonly used versions of direct simple shear test (DSS) that have been developed since the first introduction of this test by the Swedish Geotechnical Institute (SGI) in 1936 (Kjellman 1951): Cambridge type, Norwegian Geotechnical Institute (NGI) type, and stacked-ring type.

For validation of discrete element modeling (DEM) of various laboratory tests, many researchers have used idealized granular materials such as steel spheres (e.g., O'Sullivan et al. 2004, Cui and O'Sullivan 2006, and Bernhardt et al. 2016) or glass beads (e.g., Sitharam et al. 2005, Dabeet et al. 2011, Asadzadeh and Soroush 2016) that are much simpler to model compared to real soils. Regardless of the granular material tested and the laboratory test being simulated, it is of great importance that the boundary deformations in the numerical model

replicate those expected in the laboratory.

Regarding the 3D DEM simulation of direct simple shear (DSS) test, the literature differs mainly in consideration of boundary conditions. Depending on the type of the simple shear tests, researchers have numerically imposed such boundary deformation in different ways. Dabeet 2014 modeled a small-scale NGI-type simple shear test with a specimen confined by a wire-reinforced rubber membrane. They used spherical glass beads as testing materials. They modeled the lateral boundaries of the specimen as a stack of cylindrical walls in DEM. To simulate the shearing phase, they assigned constant pre-defined velocity values to each ring in a way that their movement generates a continuous and uniform simple shear deformation along the boundaries. Bernhardt et al. (2014) and Bernhardt et al. (2016) modeled a small-scale stacked ring simple shear test of steel spheres under constant stress condition. The experimental specimen was confined by a rubber membrane within a stack of rings. To make rough fixed-particle boundaries and avoid slipping and rolling of spheres along the horizontal boundaries, they used epoxy to attach particles to the top and bottom porous stones. To replicate the experimental glued particles, the particles in contact with horizontal boundaries are assigned to move with the same velocity as their adjacent horizontal boundary and their rotation is also set to zero. Bernhardt et al. (2014) stated that the velocities of the rings were updated at every 10 cycles with the target of keeping the net force very close to zero. Asadzadeh and Soroush (2016) modeled a small-scale stacked-rings simple shear test under constant stress condition using glass beads for testing materials. In their simulations, “saw-tooth configuration” was modeled for the roughness of the top and bottom boundaries, which is similar to the platens they used in experiment. In both simulation and experiment, the top boundary and its adjacent ring were stationary while the bottom boundary and its adjacent ring moved with a constant velocity. For each of the other rings in the simulation, the velocity was set independently to provide a uniform boundary shear strain.

In this study, discrete element modeling is used to investigate the level of transfer of shear deformation from the externally moving boundary into the specimen of uniform-sized chrome steel spheres in constant volume large scale stacked-ring simples shear device.

DEM MODELING

The commercially available discrete element code software PFC^{3D} 5.00 developed by Itasca Consulting Group Inc. (2014) is used to model monotonic constant volume direct simple shear test. Physical specimens of loosely packed grade 25 chrome steel spheres of 3/8 in. (9.5 mm) diameter supplied by Thompson Precision Ball are prepared and consolidated in the 12”-diameter direct simple shear device developed at the University of Michigan (Zekkos et al. 2018). The specimens are prepared within a stack of 17 Teflon-coated circular aluminum rings of 307.5 mm in diameter and 6.65 mm in thickness that have minimal friction against each other. The specimens are prepared by placing the chrome steel spheres loosely in layers using a small shovel until filling the cylindrical space confined by stacked rings and then consolidated under the specific vertical stresses of 400 kPa to achieve target void ratio between 0.652 and 0.675 at the end of consolidation. This range of void ratios correspond to a range of relative density of 45±2%, considering the minimum and maximum index void ratio of spheres packing to be 0.35 and 0.92, respectively. These values are equivalent to the minimum porosity of 0.26 for close hexagonal array packing of homogenous spheres and to the maximum porosity of 0.48 for simple cubical array packing (Smith et al. 1929).

To numerically replicate the laboratory specimen in PFC^{3D}, the bottom and top aluminum

caps are modeled as planar wall elements, and the confining rings are modeled as stacked cylindrical wall elements of the same number, diameter, and thickness as in the laboratory. This cylindrical space is then filled with the same number of spheres as in the laboratory (Figure 1). Radius expansion is used for initial preparation of the specimen (e.g., Jiang et al. 2003, Belheine et al. 2009, Gu et al. 2014, Asadzadeh and Soroush 2018, Garcia and Bray 2018). After the initial assembly, the specimen is consolidated to the target vertical stress in steps by moving the top cap vertically utilizing the servo control algorithm in PFC. To remove additional kinetic energy during the initial assembly and consolidation stages, local damping coefficient of maximum 0.1 is assigned to spheres at different points during simulation to establish equilibrium. The Hertz contact model is used in the simulations. This contact model consists of a nonlinear formulation based on an approximation of the theory of Mindlin and Deresiewicz (Mindlin and Deresiewicz 1953). The material and contact properties used in simulations are listed in Table 1. These values are either provided by the manufacturer or used by other researchers for the same material or are in the range of values for a property of a specific material.

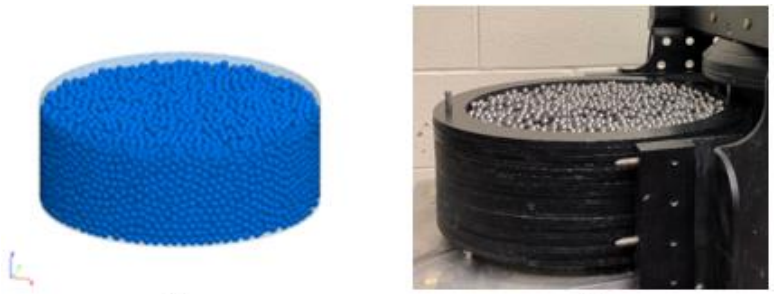

Figure 1 - (a) Numerical and (b) Experimental specimen of 10,636 chrome steel spheres

Table 1- Material and contact properties used in DEM

Parameter	Value	Reference
shear modulus-spheres	78.1 GPa	Manufacturer
Poisson's ratio-spheres	0.28	from Cui and O'Sullivan 2006
shear modulus-walls	25.9 GPa	in range for Aluminum
Poisson's ratio-walls	0.33	in range for Aluminum
density-spheres	7.83×10^3 kg/m^3	Manufacturer
inter-sphere friction coefficient	0.096	from Cui and O'Sullivan 2006
friction coefficient at ring boundaries (ring-ring and ring-sphere)	0	frictionless rings
ring mass	584 gr	Measured

For modelling the shearing stage, the bottom cap is displaced horizontally with a constant velocity of 4.8×10^{-3} m/s while the movements of the stacked rings in the simulation are set to follow the equation of motion in the direction of shearing. With a time step of average value of about 1×10^{-6} second/computational cycle, the bottom cap is displaced about 4.8×10^{-6} mm during each computational cycle. Parametric analysis has shown that the simulation response is not affected by a smaller shear rate. Moreover, the average unbalanced force ratio during the

shearing stage for this shear rate remains mostly smaller than 1×10^{-3}. Therefore, the applied shear rate assures the quasi-static condition during shearing of the simulated specimen.

In PFC, wall motion does not obey the equations of motion and they only can translate or rotate with user-defined translational velocity and angular velocity (or spin). As a result, user-defined functions are added to the sequence of operations executed during each calculation cycle. These user-defined functions for rings translational movement in direction of shear follow the same algorithm that PFC utilizes for updating the movement of the particles. In this user-defined functions, the following equation of translational motion in direction of shear for rings are solved during each calculation cycle using the second-order Velocity Verlet algorithm (Verlet 1967):

$$F_{RS} = m_R \ddot{x}_{RS}$$

where F_{RS} is the resultant force in the direction of shear acting on the ring, m_R is the mass of the ring, and $\ddot{x}_{RS}$ is the translational acceleration of the ring in direction of the shear. Since in the simulations of this study, the gravitational acceleration vector is perpendicular to the direction of shear, this parameter is not included in the equation.

Table 2- List of the numerical model groups used in the DEM analyses

Simulation Group	Name	Description
A (friction coefficient at cap boundaries = 0.125)	A-1	Bottom cap moves with a predefined velocity, and the movements of the ring follow the equation of motion in the direction of shear.
	A-2	Rings are all moving together like a rigid wall following equation of motion while bottom cap moves with a predefined velocity
	A-3	Adjacent rings to both caps are fixed to the caps, and the other rings movements follow the equation of motion in the direction of shear.
	A-4	The rotation of spheres in contact with top and bottom caps just before shearing is fixed so no rolling happens at caps during shear (sliding is allowed). The movements of all rings follow the equation of motion in the direction of shear.
	A-5	The movement (in the direction of shear) of spheres in contact with top and bottom caps just before shearing are fixed so no sliding happens at caps during shear (rolling is allowed). The movements of all rings follow the equation of motion in the direction of shear.
B (friction coefficient at cap boundaries = 1.0)	B-1	Same as in A-1.
	B-3	Same as in A-3.
	B-4	Same as in A-4.

Two groups of numerical simulations named A and B are considered. All the parameters are the same in these two groups (refer to Table 1) except the friction coefficient at contacts between steel spheres and caps. In group A, the friction coefficient between steel spheres and caps is 0.125 (corresponding to low friction angle of about 7°) while in group B, it is a high value of 1.0 (corresponding to high friction angle of 45°). Further differences among the simulations in each

group relate to how the shear stage is modeled. Table 2 summarizes these simulations with a brief description.

DEM ANALYSIS RESULTS AND DISCUSSION

To examine if the shear deformation is completely transferred from the bottom cap into the specimen, the profile of ring displacement is monitored during the simulation of shear phase. Figure 2 shows the stacked rings horizontal displacement profile for models A-1 and B-1 at two shear strain levels of 0.5% (small strain at the beginning of the shear) and 3.75% (larger strain as shearing continues). It should be mentioned that in all models regardless of whether shear deformation is completely transferred into the specimen or not, shear strain is calculated as the ratio of bottom cap displacement to the consolidated height unless stated otherwise. This does not cause any problem in comparisons between models since all the numerical specimens are generated at similar void ratios and consequently similar consolidated height. These profiles are compared to the theoretical continuous simple shear deformation at the lateral boundaries (solid line) in which the caps and rings displacement varies linearly from the corresponding displacement at the bottom cap to zero at the top cap (as shown in a small sketch in Figure 2). It should be mentioned that since at the end of consolidation (in both experimental and simulated specimen), the top cap is placed inside the most top ring, this ring remains stationary with the top cap during shear.

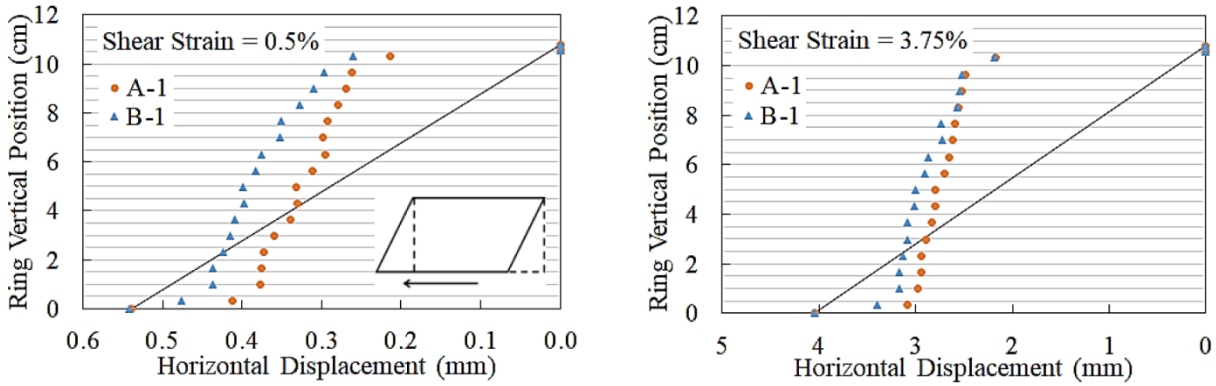

Figure 2 - Horizontal displacement of stacked rings during shear in models A-1 and B-1

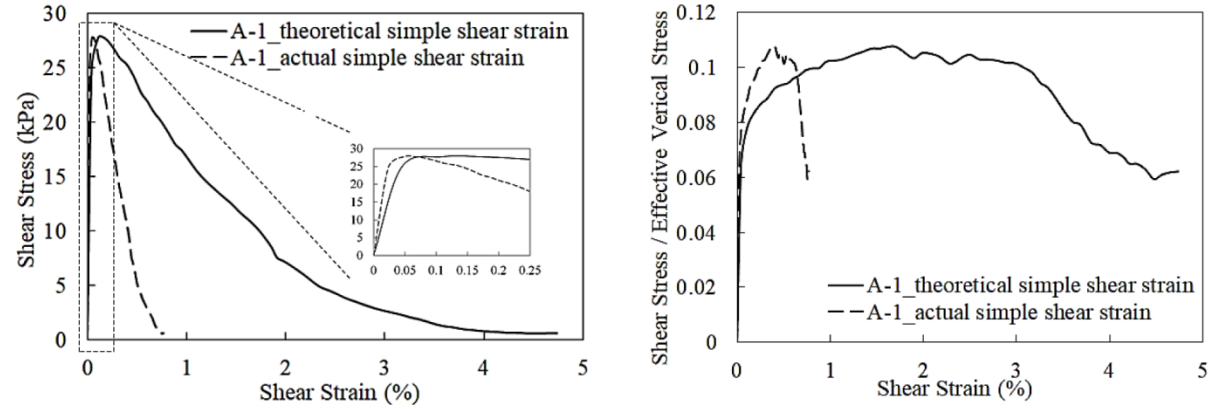

Figure 3 - Monotonic shear response in model A-1 considering actual versus theoretical simple shear strain

In Figure 2, regardless of the amount of friction at the caps, significant displacement gaps can be observed at the bottom and top caps, which can be as a result of sliding and/or rolling of particles at the boundaries. Also, the rings displacement profiles are less inclined compared to the expected inclination shown by the theoretical deformation. Figure 3 shows the comparison of shear stress-strain graphs for model A-1 by considering theoretical and actual shear strains. The actual simple shear strain of the specimen can be achieved by linear regression through the freely moving ring displacement points (not including the caps and the most top ring stuck with the top cap). Since the actual shear strain in the specimen is smaller than the theoretical one, the curved is compressed in the horizontal direction.

The other observation from Figure 2 is that for the simulated specimen, the simple shear deformation is not imposed at the boundaries. Most of the shearing happened at the interface between the steel spheres and caps and mostly the interface shear stress was captured. To reexamine this claim, the results of model A-1 are compared with model A-2 in which all the rings (except the most top ring which is stuck to the top cap) are fixed to move together as one single rigid cylindrical wall following the equations of motion while the bottom cap is moving. Figure 4a depicts the rings displacement profile in models A-1 and A-2 at two different shear strain level based on the displacement of the bottom cap. Figure 4b compares the shear response of these models. Shear responses of both models are very similar, which supports the claim that most of the shear in model A-1 happens at the interface with the caps rather than inside the specimen. The minor discrepancies between the responses can be attributed to the difference in the level of lateral restraints in these models. Because of the discrete nature of the sphere assembly, the movement of the bottom cap can cause local displacements on the adjacent spheres in contact. The propagation of these displacements in model A-1 can cause global shear deformation in the specimen as can be seen in its rings displacement while the global shear deformation is prevented in model A-2 because of constraints on the individually lateral displacement of the rings.

In models A-3 and B-3, the adjacent ring to each cap is fixed to them during the simulation. The rest of the rings move following the equation of motion. It can be observed (Figure 5) that fixing the movement of the end rings to their adjacent caps results in improvement of shear deformation transfer into the specimen. However, in both cases, this transfer is still partial, and the desired simple shear deformation is not imposed on the specimen. Figure 6 illustrates the comparison of shear stress-strain graphs in model A-3 by considering theoretical and actual shear strain values. Again, the actual shear strain values for the specimen is achieved by linear regression of the ring profile considering only free moving rings. The theoretical shear strain is calculated based on the displacement of bottom cap assuming that the shear deformation is completely transferred into the specimen and a continuous simple shear deformation is imposed on the boundaries. It confirms the previous observation that by fixing the caps to their adjacent rings the transfer of shear deformation into the specimen is improved. Since the bottom ring is externally moving with the bottom cap, the shear stress in this model is calculated by adding the total horizontal forces (in the direction of shearing) exerted on the bottom cap and the adjacent ring divided by the specimen cross-sectional area. As more shear deformation is transferred into the specimen, the simulation of shear responses better resembles the typical undrained shear behavior of loose to medium dense cohesionless granular materials (e.g., Vaid and Chern 1985; Yamsiri and Soga 2010); the shear stress increases up to a peak value followed by a strain-softening until it reaches phase transformation and after that strain hardening occurs in the specimen response.

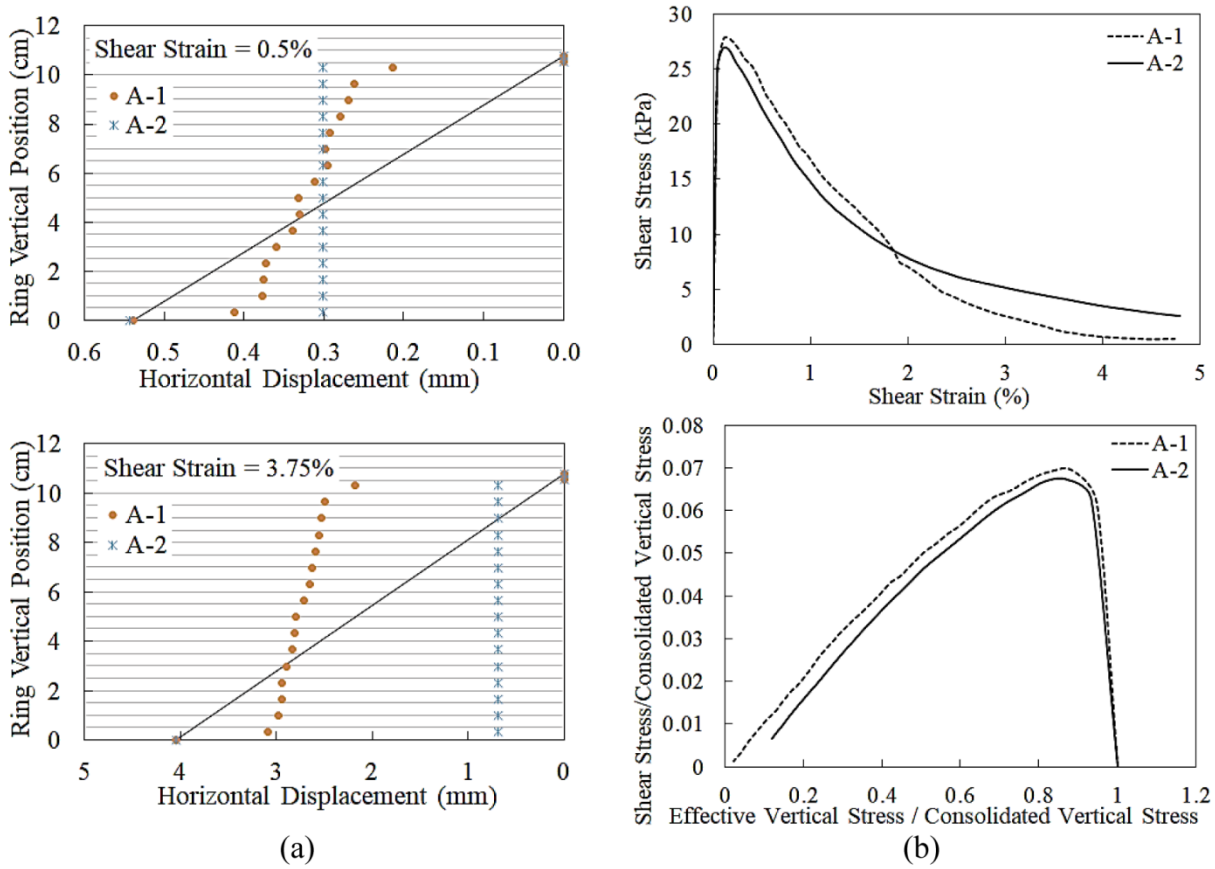

Figure 4 - (a) rings displacement profile, (b) comparison of shear responses in models A-1 and A-2

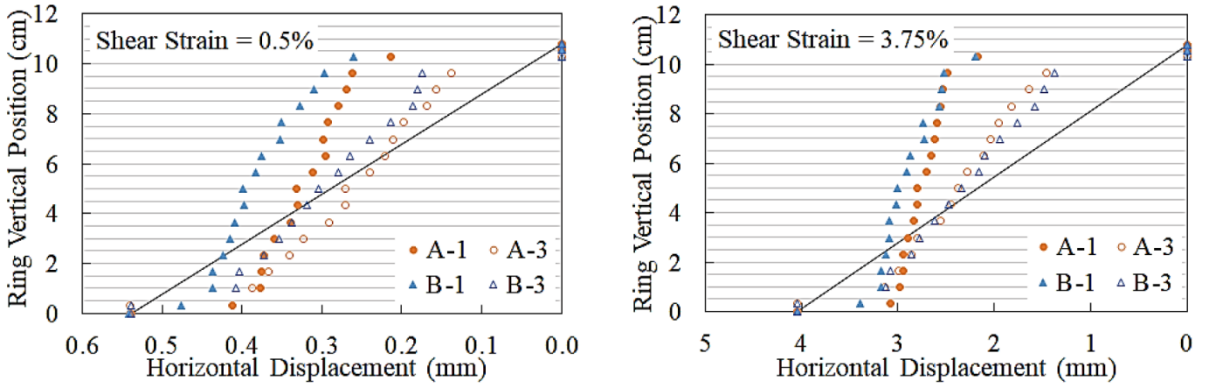

Figure 5 - Rings displacement during shear in models A-3 and B-3 compared to A-1 and B-1, respectively.

In models A-4, B-4, and A-5, all the rings move following the law of motion while some constraints are applied on the spheres in contact with the caps. In models A-4 and B-4, the spheres that are in contact with the caps at the end of the consolidation stage are identified and their rotation and spin (angular velocity) are set to zero and therefore the rolling of spheres are prevented at the caps during shear. In model A-5, sliding of spheres at the caps is prevented (instead of rolling in model A-4) by fixing the displacement of the spheres in contact with the caps at the end of the consolidation to their contacting caps. Figure 7 illustrates the rings

displacement profile for models A-4, B-4, and A-5 and their comparison with models A-1 and B-1 in which there are no constraints applied on the spheres in contact with the caps. As shown, preventing the boundary spheres at caps in model A-4 from rotating reduces the shear deformation transfer into the specimen. It reveals that fixing the rolling of the boundary spheres cannot guarantee the transfer of shear deformation into the specimen when there is not enough large friction available at caps. In model B-4, with a high friction coefficient of 1.0 (corresponding to friction angle of 45°) at caps, the resultant ring profile resembles a continuous simple shear deformation. It can also be observed in Figure 7 that preventing sliding at the caps by constraining the displacement of spheres to their contacting caps can guarantee the complete transfer of shear deformation into the specimen, even if no constraints applied to their free rotation.

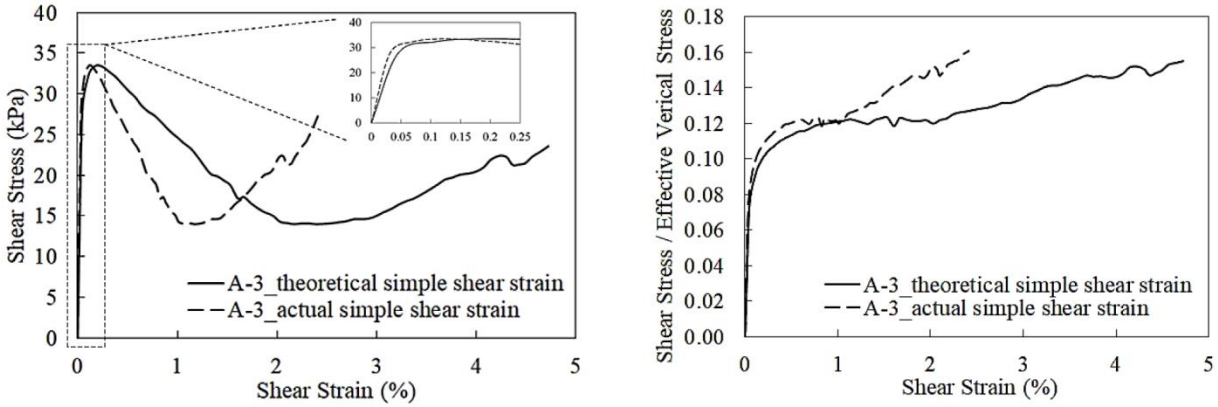

Figure 6 - Monotonic shear response in model A-3 considering actual versus theoretical simple shear strain

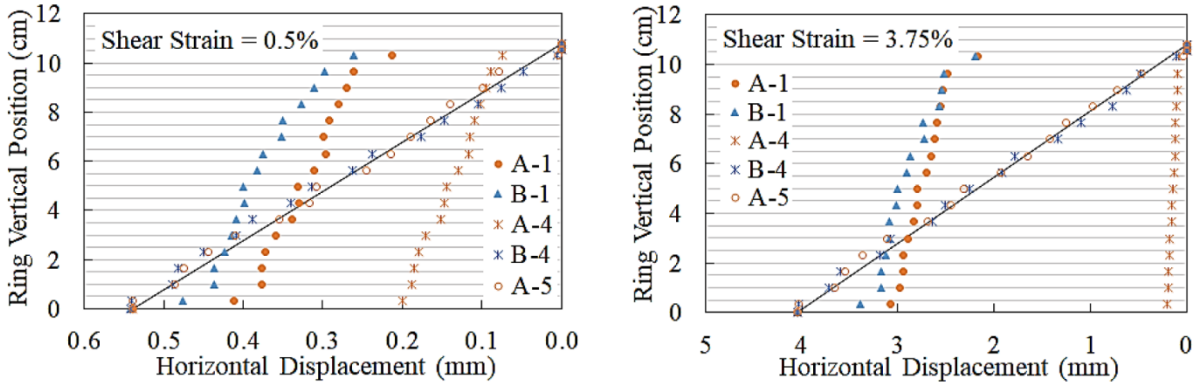

Figure 7 – Effect of preventing rolling (models A-4, B-4) or sliding (model A-5) at caps on rings displacement during shear

Therefore, in case of testing spherical-shaped granular materials with low particle frictions such as chrome steel spheres, rolling and sliding at the horizontal boundaries in stacked ring simple shear device can prevent adequate transfer of shear deformation to induce an ideal simple shear deformation in the specimen. Depending on the level of local sliding potential (at each particle-cap contact), constraining the free rotation of the boundary spheres may worsen or improve this transfer.

CONCLUSIONS

The DEM simulations of this study, by considering a realistic algorithm for modeling the movement of stacked rings, indicate that free rotation and low friction of steel spheres can prevent the complete transfer of shear deformation from the externally moving boundary into the specimen. Therefore, the simple shear deformation may not be imposed on the specimen as desired, and the experimental data of shear displacements and forces cannot be confidently used to reliably evaluate the simple shear behavior of the steel sphere assembly. Numerically examining a number of modifications for testing steel spheres in stacked-ring simple shear device, it is concluded that the steel spheres in contact with planar boundaries should be attached to them (e.g. by using glue) in order to avoid any slippage and rolling at these boundaries and obtaining reliable data from the experiments.

REFERENCES

Asadzadeh, M., and Soroush, A. (2016). "Fundamental investigation of constant stress simple shear test using DEM." *Powder Technology*, Elsevier B.V., 292, 129–139.

Asadzadeh, M., and Soroush, A. (2018). "Evaluation of stress and strain non-uniformity during cyclic simple shear test using DEM: effect of the horizontal platen asperities." *Granular Matter*, Springer Berlin Heidelberg, 20(3), 1–11.

Belheine, N., Plassiard, J. P., Donzé, F. V., Darve, F., and Seridi, A. (2009). "Numerical simulation of drained triaxial test using 3D discrete element modeling." *Computers and Geotechnics*, 36(1–2), 320–331.

Bernhardt, M. L., Biscontin, G., and O'Sullivan, C. (2014). "3D Discrete Element Method Simulations of a Laminar-Type Simple Shear Apparatus." *Geo-Congress 2014 Technical Papers*, (234 GSP), 614–623.

Bernhardt, M. L., Biscontin, G., and O′Sullivan, C. (2016). "Experimental validation study of 3D direct simple shear DEM simulations." *Soils and Foundations*, Elsevier, 56(3), 336–347.

Boulanger, R., Chan, C. K., Seed, H. B., Seed, R. B., and Sousa, J. B. (1993). "A Low-Compliance Bi-Directional Cyclic Simple Shear Apparatus." *Geotechnical Testing Journal*, 16(1), 36–45.

Budhu, M. (1988). "Failure state of a sand in simple shear." *Canadian Geotechnical Journal*, 25(2), 395–400.

Chang, W. J., Chang, C. W., and Zeng, J. K. (2014). "Liquefaction characteristics of gap-graded gravelly soils in K0 condition." *Soil Dynamics and Earthquake Engineering*, Elsevier, 56, 74–85.

Cui, L., and O'Sullivan, C. (2006). "Exploring the macro- and micro-scale response of an idealised granular material in the direct shear apparatus." *Géotechnique*, 56(7), 455–468.

Dabeet, a., Wijewickreme, D., and Byrne, P. (2011). "Discrete element modeling of direct simple shear response of granular soils and model validation using laboratory element tests." *14th Pan-Am. Conference and 64th Canadian Geotechnical conference*.

Dabeet, A. (2014). "Discrete Element Modeling of Direct Simple Shear Response of Granular Soils and Model Validation Using Laboratory Tests." PhD Dissertation, University of British Columbia.

Garcia, F. E., and Bray, J. D. (2018). "Distinct Element Simulations of Shear Rupture in Dilatant Granular Media." *International Journal of Geomechanics*, 18(9), 04018111 Int.

Gu, X., Huang, M., and Qian, J. (2014). "DEM investigation on the evolution of microstructure

in granular soils under shearing." *Granular Matter*, 16(1), 91–106.
Hubler, J. F., Athanasopoulos-Zekkos, A., and Zekkos, D. (2017). "Monotonic, Cyclic, and Postcyclic Simple Shear Response of Three Uniform Gravels in Constant Volume Conditions." *Journal of Geotechnical and Geoenvironmental Engineering*, 143(9), 04017043.
Itasca Consulting Group Inc. (2014). "PFC3D 5.00 Particle Flow Code in Three Dimensions." Itasca Consulting Group, Inc., Minneapolis, Minnesota, USA.
Jiang, M. J., Konrad, J. M., and Leroueil, S. (2003). "An efficient technique for generating homogeneous specimens for DEM studies." *Computers and Geotechnics*, 30(7), 579–597.
Kjellman, W. (1951). "Testing the Shear Strength of Clay in Sweden." *Géotechnique*, 2(3), 225–232.
Mindlin, R. D., and Deresiewicz, H. (1953). "Elastic Spheres in Contact Under Varying Oblique Forces." *Journal of Applied Mechanics*, 20, 327–344.
O'Sullivan, C., Bray, J. D., and Riemer, M. (2004). "Examination of the Response of Regularly Packed Specimens of Spherical Particles Using Physical Tests and Discrete Element Simulations." *Journal of Engineering Mechanics*, 130(10), 1140–1150.
Sitharam, T. G., Vinod, J. S., and Rothenburg, L. (2005). "Shear behavior of glass beads using DEM." *Powders and grains*, 5, 257–260.
Smith, W. O., Foote, P. D., and Busang, P. F. (1929). "Packing of homogeneous spheres." *Physical Review*, 34(9), 1271–1274.
Vaid, Y., and Chern, J. (1985). "Cyclic and monotonic undrained response of saturated sands." *in Advances in the Art ofTesting Soils Under Cyclic Conditions*, ASCE, 120–147.
Verlet, L. (1967). "Computer 'Exyeriments' on Classical Fluids. I. Thermodynamical Properties of Lennard-Jones Molecules." *Physical Review*, 159(2), 98–103.
Vucetic, M., and Dobry, R. (1988). "Degradation of marine clays under cyclic loading." *Journal of Geotechnical and Geoenvironmental Engineering*, 114(2), 133–149.
Wijewickreme, D. (2010). "Cyclic Shear Response of Low Plastic Fraser River Silt." *Proceedings of the 9th U.S. National and 10th Canadian Conference on Earthquake Engineering*.
Yamsiri, S., and Soga, K. (2010). "DEM analysis of soil fabric effects on behaviour of sand." *Géotechnique*, 60(6), 483–495.
Zekkos, D., Athanasopoulos-Zekkos, A., Hubler, J., Fei, X., Zehtab, K. H., and Allen Marr, W. (2018). "Development of a large-size cyclic direct simple shear device for characterization of ground materials with oversized particles." *Geotechnical Testing Journal*, 41(2), 263–279.